Electronic Supplementary Material (ESI) for Materials Advances.

Fabrication of $Mo_{1.33}CT_z$ (MXene)-Cellulose Freestanding Electrodes for Supercapacitor Applications

Ahmed S. Etman[1*], Joseph Halim[1], Johanna Rosen[1*]

[1]*Department of Physics, Chemistry and Biology (IFM), Linköping University, SE-58183, Linköping, Sweden*

Email: ahmed.etman@liu.se; johanna.rosen@liu.se

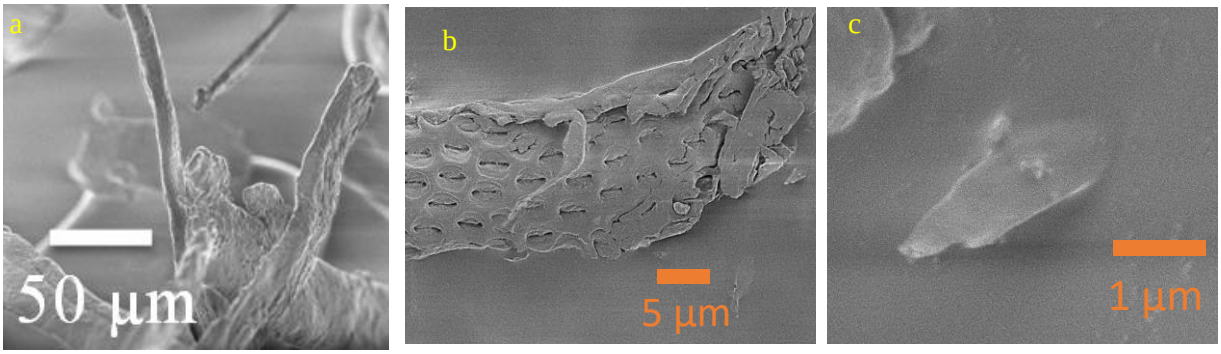

Figure S1. Morphology of cellulose before and after TBAOH treatment: (a) SEM image of the pristine cellulose powder. (b) and (c) Morphology of cellulose after sonication with TBAOH for 20 minutes.

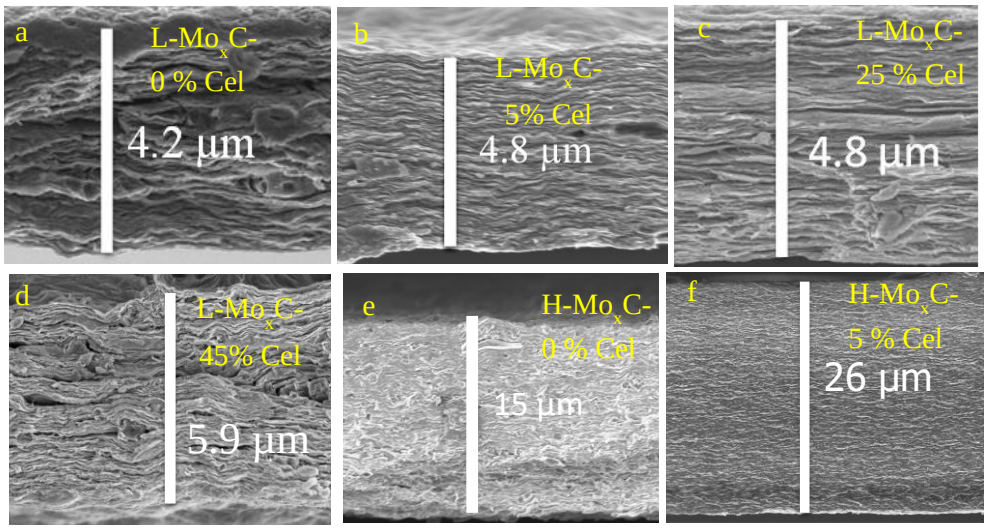

Figure S2. SEM cross-section of $Mo_{1.33}CT_z$ -cellulose films: (a), (b), (c) and (d) low loading MXene films with 0%, 5%, 25%, and 45% cellulose content, respectively. (d) and (e) High loading MXene films with 0% and 5% cellulose content.

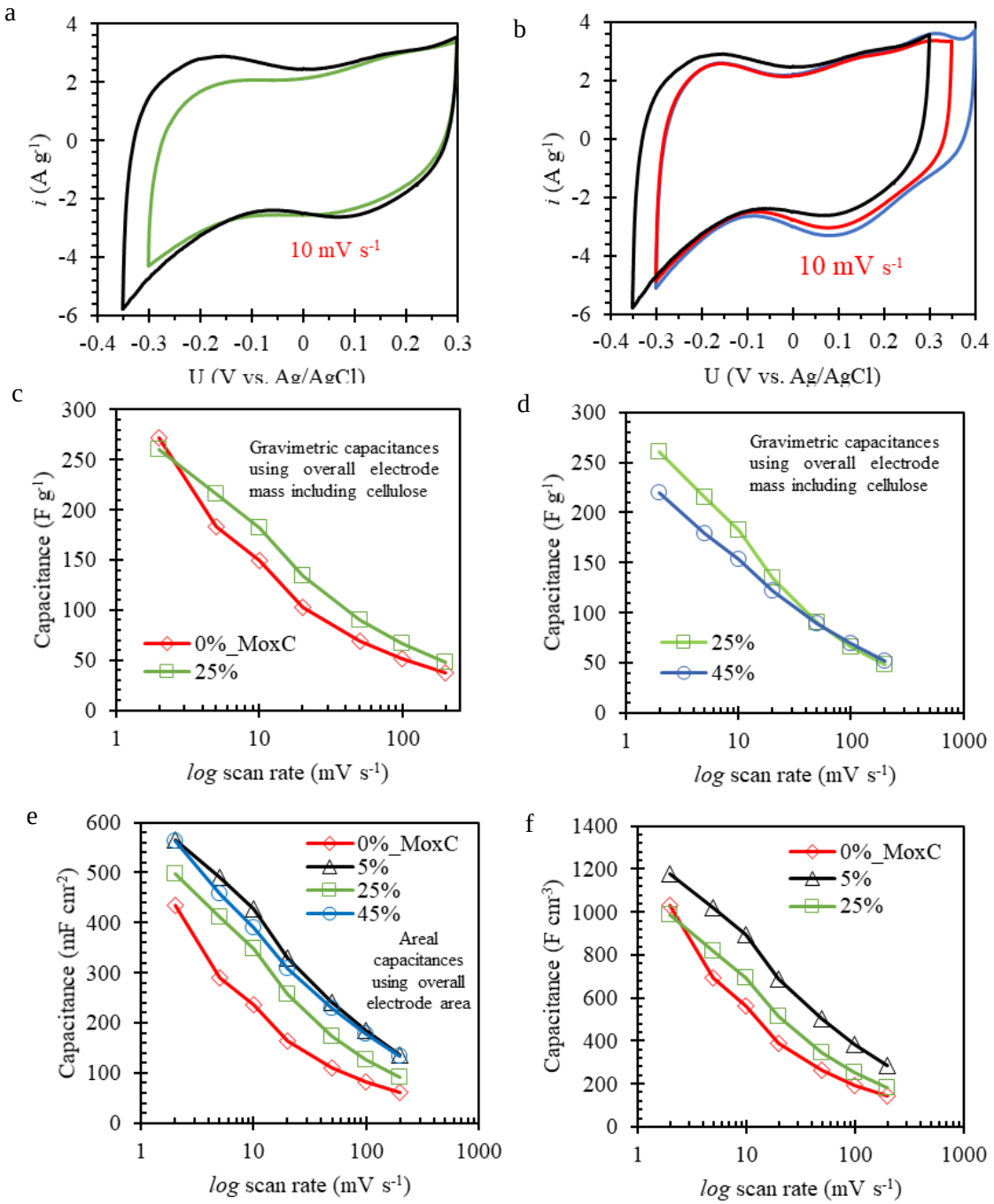

Figure S3. (a) and (b) CVs at scan rate of 10 mV s^{-1} using different upper and lower cut-off potentials in order to find the optimum cycling potential window. (c) Variation of the gravimetric specific capacitance with the scan rates for L-Mo_xC-0% Cel (red diamonds) and L-Mo_xC-25% Cel (green squares) electrodes. (d) Variation of the gravimetric specific capacitance with the scan rates for L-Mo_xC-45% Cel (blue circles) and L-Mo_xC-25% Cel (green squares) electrodes. The mass normalization in (c) and (d) was done using the overall electrode mass including cellulose. (e) and (f) Variation of the areal and volumetric capacitances, respectively, with the scan rates for L-Mo_xC-0% Cel (red diamonds), L-Mo_xC-5% Cel (black triangles), L-Mo_xC-25% Cel (green squares) and L-Mo_xC-45% Cel (blue circles) electrodes.

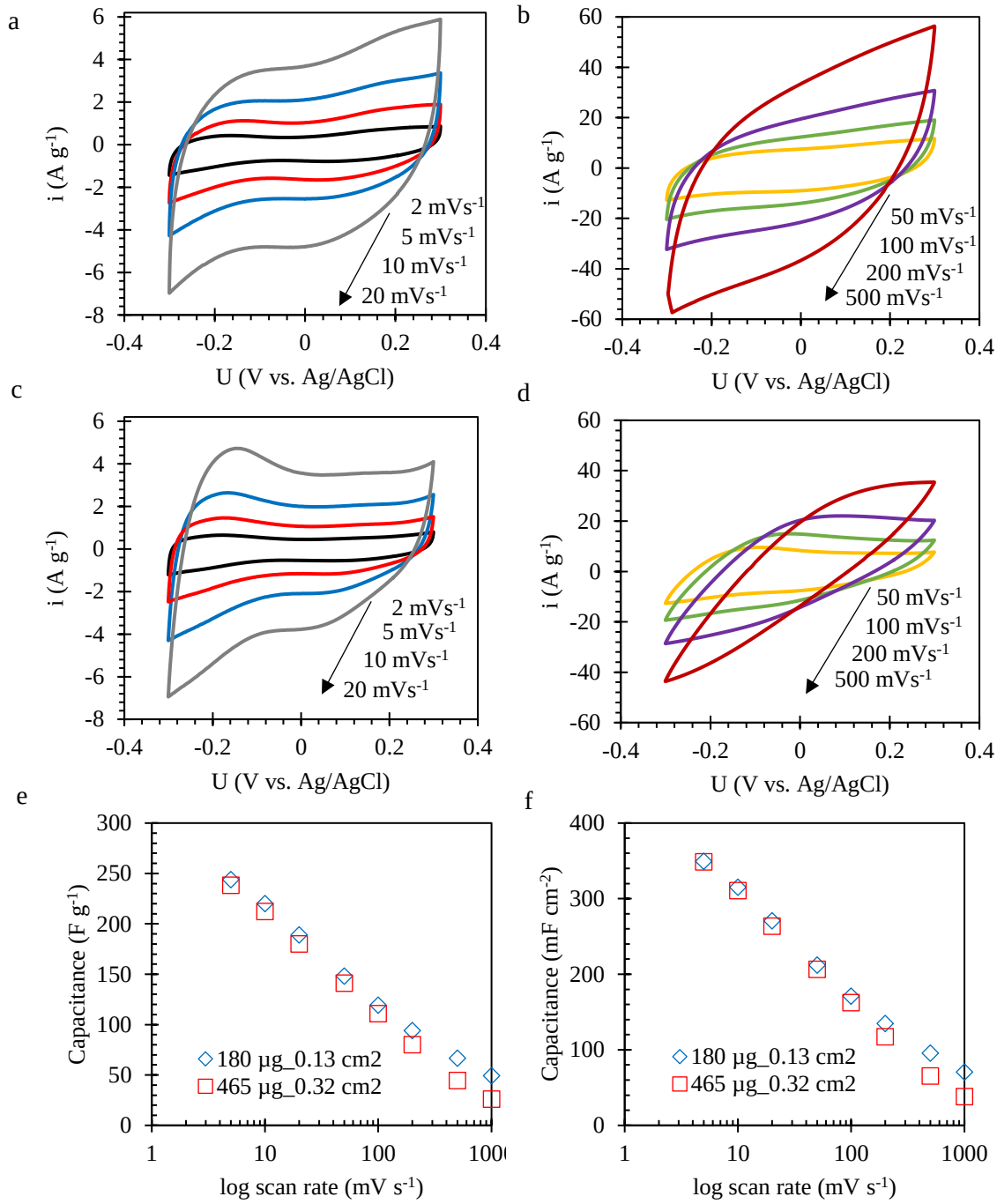

Figure S4. Comparison of the electrochemical behavior for electrodes with different dimensions: (a) and (b) CVs of L-Mo_xC-25% Cel with area 0.13 cm^2 at different scan rates. (c) and (d) CVs of L-Mo_xC-25% Cel with area 0.32 cm^2 at different scan rates. (e) and (f) variation of the gravimetric and areal capacitances, respectively, with the scan rates for L-Mo_xC-25% Cel electrodes with area 0.13 (blue diamonds) and 0.32 cm^2 (red diamonds).

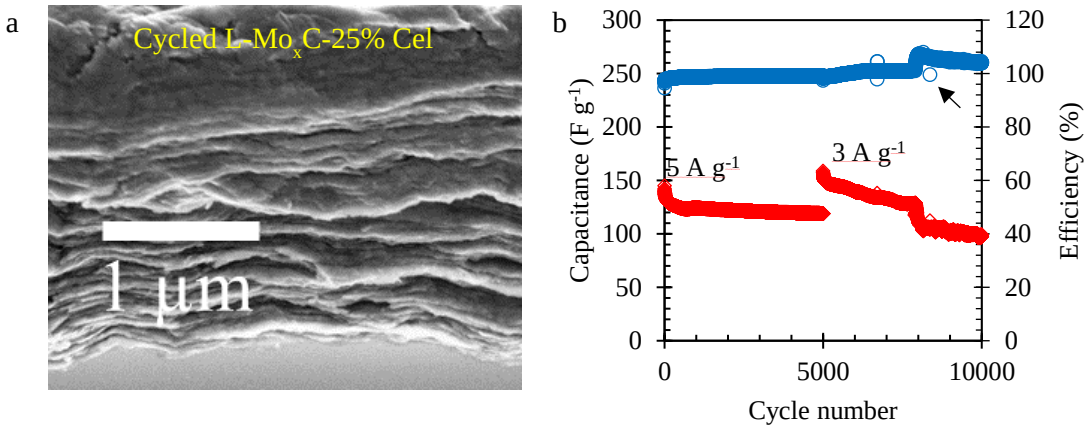

Figure S5. (a) Morphology of Mo_xC-25% Cel after long term cycling (30 000 cycles). (b) Long-term cycling of the L-Mo_xC-5% Cel (cellulose loading 0.10 mg cm^{-2}) showing its stable behavior for about 8000 cycles.

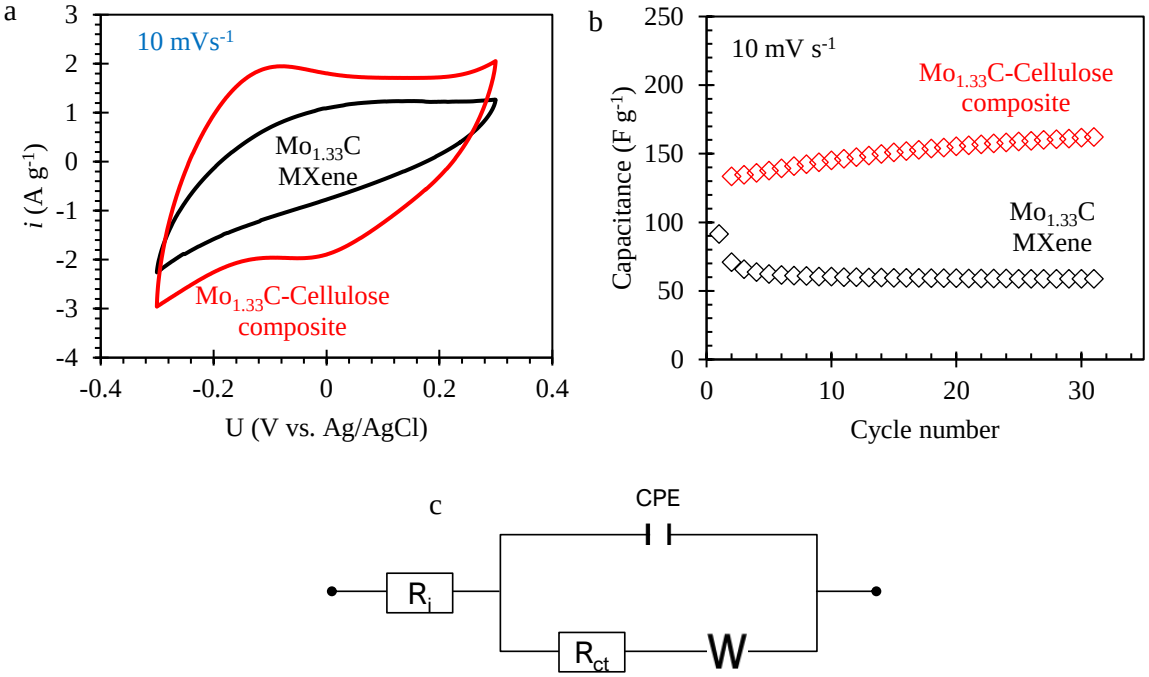

Figure S6. Comparison of electrochemical performance for electrodes with high MXene loading in the presence and absence of cellulose: (a) 30th cycle of CVs at scan rate 10 mV s^{-1} for H-Mo_xC-5%Cel (red curve) and H-Mo_xC 0% Cel (black curve). (b) Variation of the discharge capacitance with the cycle number for the initial CVs cycles at scan rate 10 mV s^{-1}, H-Mo_xC-5%Cel (red diamonds) and H-Mo_xC 0% cel (black diamonds). (c) The equivalent circuit model for the Nyquist plots in Figure 5c and d.

Table S1. Summary of the gravimetric and volumetric capacitance values of $Mo_{1.33}CT_z$-cellulose electrodes with different cellulose content and MXene loading:

Sample	Cyclic voltammetry			Galvanostatic charge-discharge		Film Thickness (µm)	Overall circular electrode mass (4 mm diameter) (µg)
	Scan rates (mV s^{-1})	Gravimetric capacitance (F g^{-1})	Volumetric capacitance (F cm^{-3})	Current density (A g^{-1})	Gravimetric capacitance (F g^{-1})		
L-Mo_xC-0% Cel	2	272	1032	0.5	329	4.2	200
	10	149	565	3	107		
	50	69	262	5	71		
	100	51	193	10	41		
L-Mo_xC-5% Cel	2	267	1178	0.5	324	4.8	280
	10	202	892	3	170		
	50	114	502	5	135		
	100	87	384	10	93		
L-Mo_xC-25% Cel	2	347	990	0.5	390	4.8	240
	10	243	695	3	218		
	50	120	343	5	163		
	100	88	252	10	101		
L-Mo_xC-45% Cel	2	400	1102	0.5	442	5.9	310
	10	279	767	3	261		
	50	163	448	5	205		
	100	126	347	10	146		
H-MoxC-5% Cel	2	266	529	0.5	300	26	690
	10	162	323	3	249		
	50	85	169	5	103		
	100	58	116	10	54		

Table S2. Comparison of the electrochemical performance of the $Mo_{1.33}CT_z$-cellulose electrodes with other state-of-the-art of Ti and Mo based MXene electrodes:

Sample	Scan rate /current density	Gravimetric capacitance (F g^{-1})	Areal capacitance (mF cm^{-2})	Mass loading (mg cm^{-2})	Electrolyte	Capacity retention	Ref.
$Ti_3C_2T_z$@carbon-fiber	10 mV s^{-1}	400	320	0.8	1M H_2SO_4	98% after 20 000 cycles	1
$Ti_3C_2T_z$@carbon-fiber	10 mV s^{-1}	200	416	2.6	1M H_2SO_4	98% after 20 000 cycles	1
$Ti_3C_2T_z$(97%)@carbon-nanotube yarn	2 mA cm^{-2}	428	3188	-	3M H_2SO_4	95% after 10 000 cycles	2
MXene aerogel	2 mV s^{-1}	67	1012	15	1M KOH	84% after 5 000 cycles (asymmetric device)	3
$Ti_3C_2T_z$/Ag nanoparticle	5 mA cm^{-2}	78	1173	15	1M Na_2SO_4	78% after 15 000 cycles	4
$Ti_3C_2T_z$/bacterial-cellulose	3 mA cm^{-2}	416	2084	5	3M H_2SO_4	96% after 10 000 cycles	5
$Ti_3C_2T_z$/20%-cellulose nanofibers	5 mV s^{-1}	285	600	1.6	3M H_2SO_4	10 000 cycles	6
Mo_2CT_z(2μm-thick)	2 mV s^{-1}	196	-	0.6	1M H_2SO_4	10 000 cycles	7
$Mo_{1.33}CT_z$(3μm-thick)	2 mV s^{-1}	339	-	-	1M H_2SO_4	84% after 10 000 cycles	8
$Mo_{1.33}CT_z$/PEDOT:PSS (2μm-thick)	2 mV s^{-1}	452	-	-	1M H_2SO_4	90% after 10 000 cycles (symmetric device)	9
H-$Mo_{1.33}CT_z$-5% cellulose (26μm-thick)	2 mV s^{-1}	266	1400	5.2	1M H_2SO_4	95% after 30 000 cycles	This work
L-Mo_xC-45% cellulose (5.9μm-thick)	2 mV s^{-1}	440	563	1.6	1M H_2SO_4	95% after 30 000 cycles	This work

References:

1 Q. Jiang, N. Kurra, M. Alhabeb, Y. Gogotsi and H. N. Alshareef, *Adv. Energy Mater.*, 2018, **8**, 1703043.

2 Z. Wang, S. Qin, S. Seyedin, J. Zhang, J. Wang, A. Levitt, N. Li, C. Haines, R. Ovalle-Robles, W. Lei, Y. Gogotsi, R. H. Baughman and J. M. Razal, *Small*, 2018, **14**, 1802225.

3 L. Li, M. Zhang, X. Zhang and Z. Zhang, *J. Power Sources*, 2017, **364**, 234–241.

4 L. Li, N. Zhang, M. Zhang, L. Wu, X. Zhang and Z. Zhang, *ACS Sustain. Chem. Eng.*, 2018, **6**, 7442–7450.

5 Y. Wang, X. Wang, X. Li, Y. Bai, H. Xiao, Y. Liu, R. Liu and G. Yuan, *Adv. Funct. Mater.*, 2019, **29**, 1900326.

6 W. Tian, A. VahidMohammadi, M. S. Reid, Z. Wang, L. Ouyang, J. Erlandsson, T. Pettersson, L. Wågberg, M. Beidaghi and M. M. Hamedi, *Adv. Mater.*, 2019, **31**, 1902977.

7 J. Halim, S. Kota, M. R. Lukatskaya, M. Naguib, M.-Q. Zhao, E. J. Moon, J. Pitock, J. Nanda, S. J. May, Y. Gogotsi and M. W. Barsoum, *Adv. Funct. Mater.*, 2016, **26**, 3118–3127.

8 Q. Tao, M. Dahlqvist, J. Lu, S. Kota, R. Meshkian, J. Halim, J. Palisaitis, L. Hultman, M. W. W. Barsoum, P. O. Å. O. Å. Persson and J. Rosen, *Nat. Commun.*, 2017, **8**, 14949.

9 L. Qin, Q. Tao, A. El Ghazaly, J. Fernandez-Rodriguez, P. O. Å. Persson, J. Rosen and F. Zhang, *Adv. Funct. Mater.*, 2018, **28**, 1703808.